Materials and Design 40 (2012) 52–58

Contents lists available at SciVerse ScienceDirect

Materials and Design

journal homepage: www.elsevier.com/locate/matdes

Technical Report

Metallurgical and mechanical characterization of stir cast AA6061-T6–AlN_p composite

B. Ashok Kumar [a,*], N. Murugan [b,1]

[a] Department of Mechanical Engineering, Faculty of Engineering, Erode Builder Educational Trust's Group of Institutions, Nathakadaiyur, Kangayam 638 108, Tirupur District, Tamil Nadu, India
[b] Department of Mechanical Engineering, Coimbatore Institute of Technology, Coimbatore 641 014, Tamil Nadu, India

ARTICLE INFO

Article history:
Received 12 January 2012
Accepted 20 March 2012
Available online 30 March 2012

ABSTRACT

An attempt has been made to manufacture aluminium (6061-T6) matrix composites reinforced with aluminium nitride particles (AlN_p) of size 3–4 μ using indigenously developed modified stir casting method with bottom pouring arrangement in controlled argon environment. To improve the wettability of AlN_p with molten Al matrix, 2% Mg has been added. AA6061–AlN_p composites have been successfully produced at different weight percentages (viz 0, 5, 10, 15 and 20) of AlN_p and their metallurgical and mechanical properties have been analysed. Macrohardness, microhardness, Yield strength and ultimate tensile strength of the composite have improved with the addition of AlN_p in the Al matrix. Optical and SEM micrographs reveal the homogeneous distribution of reinforcement particles in the matrix and X-ray diffraction patterns ensure the dispersion of AlN_p reinforcement in AA6061 matrix.

1. Introduction

In day to day life, usage of aluminium matrix composites (AMCs) is enormously increasing due to its high strength-to-weight ratio and enhanced mechanical and thermal properties. AMCs have become very attractive for automotive and aerospace applications [1–4]. Thus particulate form of reinforcement present in the composites exhibits an isotropic property when compared with other geometries of reinforcement such as fibre and flake. Fibre and flake composites are generally anisotropic. The advantages of particulate composites are improved strength, increased operating temperature, oxidation resistance, easy to produce, etc. [5].

Al–SiC and Al–AlN_p composites are widely used in microelectronic devices. Although the thermal conductivity of AlN (175 W/m K) is less than SiC (250 W/m K), AlN is chemically more stable than SiC. Aluminium does not react with AlN [6] whereas in Al–SiC composites Al_4C_3 phase is formed by the reactions of Al with SiC and degrades the mechanical properties of Al–SiC composite [7,8]. AlN has good compatibility with Al alloy, excellent thermophysical properties, good interfacial adherence without interfacial reaction [6], high specific strength & stiffness, high thermal conductivity, high electrical resistivity, low dielectric constant and tailorable coefficient of thermal expansion. Thus Al–AlN_p composite is an ideal candidate material for electronic packaging materials [9,10]. AA6061 alloy is used as matrices, as they offer good thermal conductivity, low density, easy to process, good castability and weldability compared with other high thermal conductivity matrix metal like copper [11].

AlN_p reinforced aluminium matrix composite is fabricated through pressure infiltration of liquid aluminium [12,13], powder metallurgy [14], powder injection moulding process [15], squeeze casting technique [7,8,10], in situ reaction [16–18] and stir casting method [19,20]. Even though AMCs are fabricated by several methods as mentioned above, the stir casting method is currently employed commercially. Advantages of stir casting method include simple, flexible, economical, suitable for mass production and production of complex profiled composite components without damaging the reinforcement particles. Due to these salient features of stir casting method, recently many attempts have been made to produce different composites using this method [19–23]. Some of the difficulties encountered in the fabrication of AMCs in stir casting method are achieving a uniform distribution of the reinforcement particles in the matrix, wettability between the matrix alloy and reinforcement particles, porosity in the cast AMCs and chemical reactions between the reinforcement particles and matrix alloy.

Homogenous distribution, wetting of reinforcement particles with the matrix and minimized porosity in the cast can be achieved by choosing appropriate process parameters such as molten metal temperature, uniform feed rate of reinforcement

* Corresponding author. Tel.: +91 4257 241935, mobile: +91 9942699429; fax: +91 4257 242007.
E-mail addresses: ashokbkumar@yahoo.com (B. Ashok Kumar), murugan@cit.edu.in (N. Murugan).
[1] Tel.: +91 422 2574071/2574072, mobile: +91 9751824123; fax: +91 422 2575020.

0261-3069/$ - see front matter © 2012 Elsevier Ltd. All rights reserved.
http://dx.doi.org/10.1016/j.matdes.2012.03.038

Table 1
Chemical composition of AA6061-T6 alloy matrix.

Element	Mg	Si	Fe	Mn	Cu	Cr	Zn	Ni	Ti	Al
wt%	0.9	0.64	0.26	0.1	0.21	0.05	0.04	0.02	0.01	Balance

Fig. 1. The manufactured typical AA6061–AlN_p composites.

particles, incorporation time and stirring speed [23,24]. Nassaj et al. [19] stated that by adding 2% of Mg, incorporation time was reduced and wettability of the AlN_p with Al melt was improved by which the mechanical properties of the Al–AlN_p composite were increased.

Limited research work has been carried out on the mechanical and the metallurgical properties of stir cast Al–AlN_p composites containing wide range of reinforcement. In this paper, the metallurgical and the mechanical characterization of AA6061–AlN_p composite (by varying AlN_p range from 0% to 20% by weight) produced in an inert atmosphere using a modified stir casting technique with the bottom pouring arrangement are presented.

2. Experimental procedure

A cleaned extruded aluminium alloy (AA6061-T6) rods of 25 mm diameter were placed inside the stainless steel crucible of electric stir casting furnace with bottom pouring attachment. The chemical composition of AA6061 rods is presented in Table 1. In order to avoid any contaminations at high temperatures, inner side of the stainless steel crucible and stainless steel stirrer were coated. Temperature of the electric furnace was set to 1000 °C. When the temperature of the furnace reached 650 °C, argon gas was supplied into the crucible at a constant flow rate of 2 lpm to avoid the reaction of matrix with the atmospheric air. By the time the temperature reached 1000 °C, 2% magnesium of total weight of the composite to be produced was added to the melt to increase the wettability of AlN_p with Al alloy [19,20]. A stainless steel stirrer coupled with electric motor was immersed into the molten aluminium alloy and stirred at a constant speed of 450 rpm to form a vortex. Stirring was carried out to facilitate both incorporation and uniform distribution of the reinforcement (AlN_p) in the molten aluminium alloy [20]. Proper stirring speed is necessary to avoid excessive gas content which will form due to over agitation of melts and lead to unacceptable porosity in the cast [24].

A predetermined quantity of preheated AlN_p at 750 °C (of size 3 to 4 μ and purity of more than 99.6%) was added into the molten matrix at the side of the vortex. AlN_p particles were incorporated into the melt for 260 s. The mixture of molten aluminium and AlN_p were further stirred for 1200 s before pouring into a preheated permanent mould at 300 °C through the bottom pouring arrangement. Argon was supplied until the entire melt was poured into the permanent mould. The composites were allowed to solidify in atmospheric air and were taken out from the mould after solidification. Similarly AA6061–AlN_p composites containing different weight percentages of (ranging from 0 to 20) AlN_p were produced. The manufactured AA6061–AlN_p composites are presented in Fig. 1.

Specimens of required size were cut from the cast composite to carry out the metallurgical and the mechanical characterization. Standard metallographic procedure was adopted to prepare the specimens for optical, SEM and EDAX analysis. SEM and EDAX analysis were carried out by using a scanning electron microscope

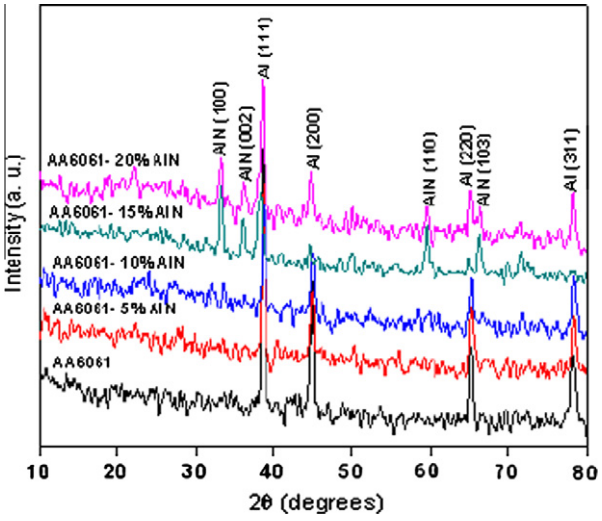

Fig. 3. The XRD patterns of fabricated AA6061–AlN_p composites.

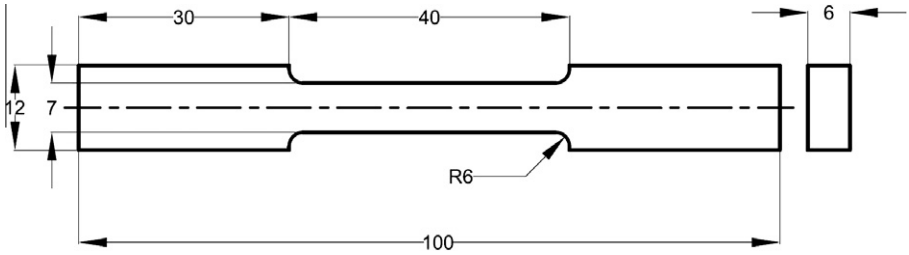

Fig. 2. The dimensions of the tensile specimen as per ASTM E8 M-04 standard.

(SEM) attached with energy dispersive spectroscope (JEOL-JSM-6390). X-ray diffraction patterns (XRD) were recorded using a Panalytical X-ray diffractometer. The polished specimens were etched with colour etchant containing 1 g of sodium hydroxide (NaOH) and 4 g of potassium permanganate ($KMnO_4$) in 100 ml distilled water for metallographic study. The microstructure was observed using an optical microscope (OLYMPUS-BX51 M) and photomicrographs of composites containing various weight percentages of reinforcement are presented in Fig. 4a–f.

The macrohardness was measured using a Brillnell hardness tester (model 7KB3000) at a load of 500 kg applied for 15 s at eight different locations on all samples. The microhardness of the etched AA6061–AlN_p composites was measured using a microhardness tester (MITUTOYO-MVK-H1) at a load of 500 g applied for 15 s at twenty different locations on all samples. The average values of macrohardness and microhardness were recorded. Three tensile specimens as per ASTM E8 M-04 standard as shown in Fig. 2 were prepared from each (% of reinforcement) cast composite [25]. The ultimate tensile strength (UTS) was estimated using a Computerized Universal Testing Machine (HITECH TUE-C-1000) and its average values were recorded.

3. Results and discussions

AA6061 alloy matrix reinforced with AlN_p composites were successfully fabricated by using the modified stir casting method with bottom pouring arrangement. The metallurgical and the mechanical characterization of fabricated AA6061–AlN_p composites are discussed below.

3.1. X-ray diffraction analysis of A6061–AlN_p composites

Fig. 3 shows the XRD patterns obtained from the fabricated composites which reveal the presence of AlN_p. The peaks of AlN are distinctly clear and they increase with the increase in AlN_p content while the peaks of AA6061 decrease. It is also interesting to note that the peaks of AA6061 in the composite are slightly shifted to lower 2θ when compared to that of AA6061 alloy. The XRD patterns also indicate that there is no formation of intermetallic compounds resulting from the reaction of AlN_p with AA6061alloy matrix. From the XRD patterns, it is clear that AlN_p are thermodynamically stable at a fabrication temperature of 1000 °C.

3.2. Evaluation of microstructure of AA6061–AlN_p composites

Fig. 4 shows the microstructures of fabricated AA6061 alloy matrix as well as AA6061 alloy matrix reinforced with AlN_p composites. Microstructure of cast AA6061 alloy matrix is presented in Fig. 4a which reveals the formation of α-aluminium dendritic network structure which is formed due to the supercooling of composite during solidification. Precipitation of Mg_2Si is also visible in the microstructure.

Fig. 4b–f shows the microstructure of AA6061–AlN_p composites containing different weight percentages of AlN_p reinforcement. Microstructures of the composites presented in Fig. 4b–e clearly

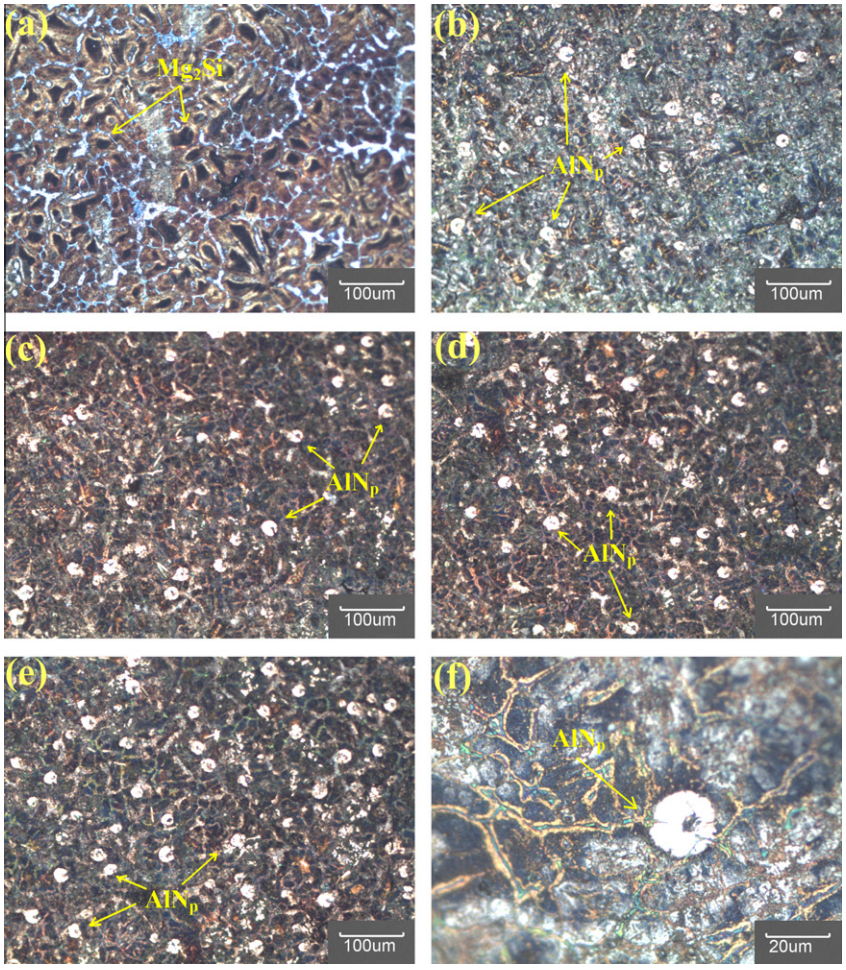

Fig. 4. The optical photomicrographs of AA6061–AlN_p composites containing: (a) 0% AlN_p, (b) 5% AlN_p, (c) 10% AlN_p, (d) 15% AlN_p, (e) 20% AlN_p, and (f) 5% AlN_p.

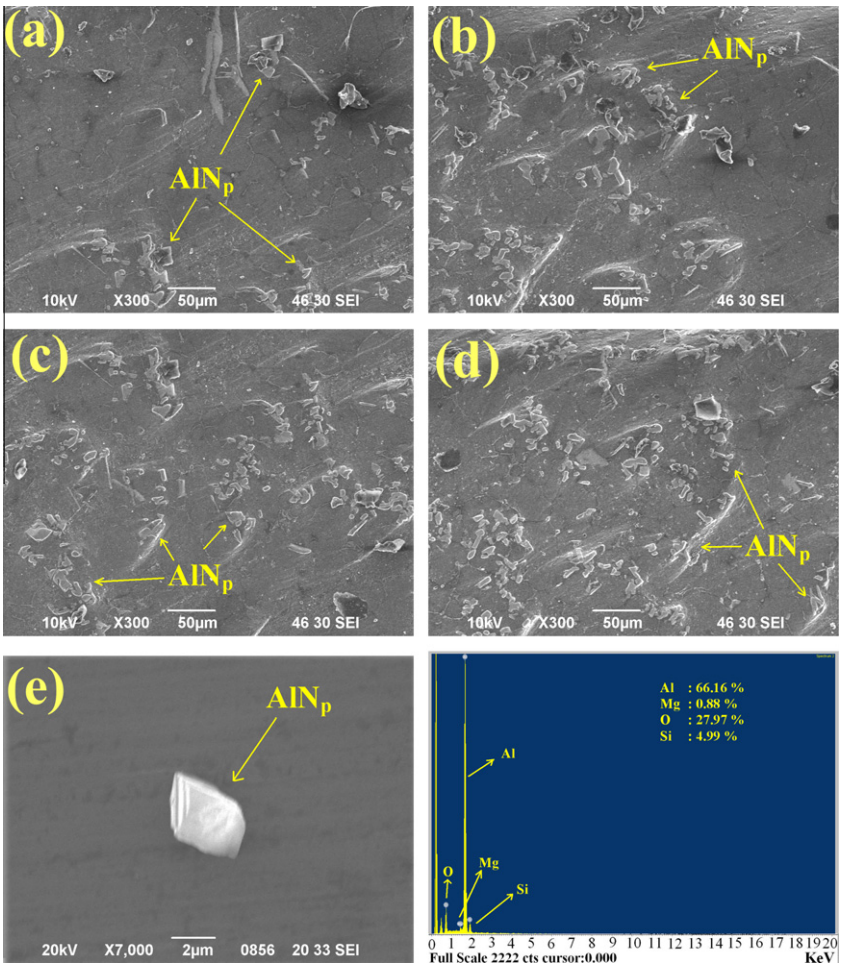

Fig. 5. The SEM micrographs of AA6061–AlN_p composites containing: (a) 5% AlN_p, (b) 10% AlN_p, (c) 15% AlN_p, (d) 20% AlN_p, (e) 5% AlN_p, and (f) EDAX analysis of AA6061–AlN_p composites containing 20% AlN_p.

reveals the homogeneous distribution of the AlN_p in the Al alloy matrix and there is no evidence of porosity and cracks in the castings. This might be related to proper process parameters employed for the production of castings. During solidification of AA6061–AlN_p composite, AlN_p are rejected in the direction of refined α-Al grains. Refinement of α-Al grains may be due to AlN_p themselves, which act as nucleus on which the α-aluminium grains solidify and AlN_p offer resistance to the growing α-Al phase during the solidification process. Fig. 4c shows the precipitation of Mg_2Si. The sources for the formation of Mg_2Si are addition of Mg in molten Al alloy matrix and Mg and Si are already present in the AA6061 alloy as major constituent.

From the SEM micrographs, it is clear that AlN_p are clustered in a uniform manner and distributed homogeneously in the matrix. Hence, appearance of single particles in the optical photomicrographs contain cluster of AlN_p. It is also evident from the photomicrographs that cluster of AlN_p in the matrix are spherical shape. Fig. 4f shows the clear interface between the Al alloy matrix and AlN_p reinforcement.

A small amount of magnesium aluminate (spinel) $MgAl_2O_4$ is formed in the matrix during the process according to the following reaction [19].

$$3Mg + 4Al_2O_3 \rightarrow 3MgAl_2O_4 + 2Al \quad (1)$$

Formation of magnesium aluminate is confirmed in the EDAX analysis which is presented in Fig. 5f. Source of oxygen for the above reaction is the oxide layer formed over the molten Al alloy matrix. Since an inert atmosphere is maintained at the top of the molten matrix, constant motorized stirring action is carried out during the incorporation of AlN_p in the matrix and molten metal is poured through bottom of the crucible, there is no formation of magnesium aluminate at the interface of matrix and AlN_p reinforcement.

Fig. 5a–d shows the SEM micrographs of fabricated AA6061–AlN_p composites containing 5% AlN_p, 10% AlN_p, 15% AlN_p and 20% AlN_p respectively. SEM micrographs show the uniform distribution of AlN_p reinforcement in the AA6061 alloy matrix. The SEM micrograph presented in Fig. 5e reveals a clear interface between AA6061 alloy matrix and AlN_p, which is due to the absence of interfacial reaction between matrix and the reinforcement. The addition of magnesium enhances the wettability between AlN_p and AA6061 alloy matrix which results in good bonding between AlN_p and AA6061 alloy matrix.

3.3. Evaluation of mechanical properties

Fig. 6 shows the average macrohardness and microhardness of AA6061–AlN_p composites. The macrohardness of AA6061–20% AlN_p composite is 79 BHN which is 107.89% greater than AA6061 matrix. Similarly microhardness of AA6061–20% AlN_p composite is 91 VHN which is 106.81% greater than AA6061 matrix. Both macro and microhardnesses of AA6061–AlN_p composites linearly increase with the addition of AlN_p due to the presence of hard AlN_p in AMCs.

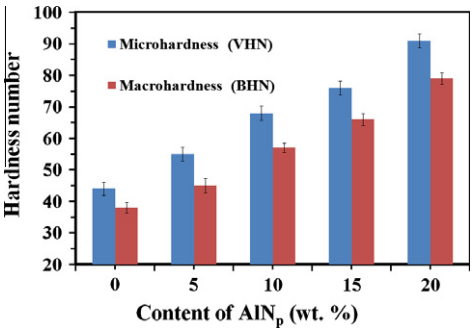

Fig. 6. Effect of weight percentage of AlN_p on microhardness and macrohardness of AA6061–AlN_p composites.

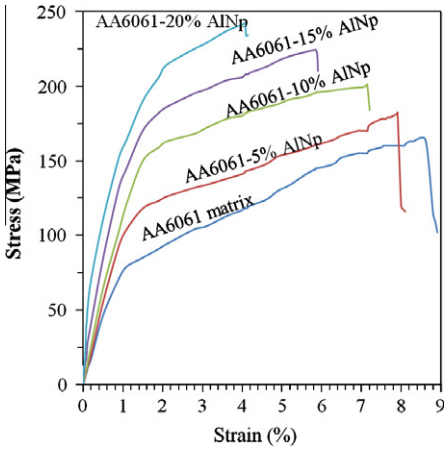

Fig. 7. Effect of weight percentage of AlN_p on stress strain curve of AA6061–AlN_p composites.

Fig. 7 reveals the typical engineering stress strain diagrams of AA6061 matrix and AA6061–AlN_p composites obtained by tensile test conducted at room temperature. The average Yield strength measured at 0.2% offset, UTS and % elongation of AA6061–AlN_p composites with various wt% of AlN_p are presented in Fig. 8. Both Yield strength and UTS are increased by the addition of AlN_p. But % elongation of the AMC decreases when the amount of AlN_p increases. Yield strength of AA6061–20% AlN_p composite is 158 MPa which is 95.12% greater than AA6061 matrix. UTS of the AA6061–20% AlN_p composite is 241 MPa which is 46.95% greater than AA6061 matrix alloy. An increase in volume fraction of low coefficient of thermal expansion reinforcement material in the higher coefficient of thermal expansion matrix changes the microstructural characteristics of the metal matrix with a concomitant contribution to increasing strength. As such, an increase in the volume fraction of the reinforcing ceramic particulate results in an increase in dislocation density around the reinforcement particles during solidification [26], reduction in grain size, and an overall reduction in the substructure. The above microstructural changes tend to increase the resistance offered to the motion of both microscopic and macroscopic level dislocations under the influence of a far-field stress [27]. Accordingly, an increase of wt% of AlN_p reinforcement in the AMCs increases the magnitude of resistance offered to the motion of both microscopic and macroscopic level dislocations. As a result macrohardness, microhardness and UTS increase with the increase in wt% of AlN_p reinforcement. Clear interface noticed between the matrix and AlN_p reinforcement and uniform distribution of AlN_p reinforcement increase the load bearing capacity of the composite [28].

The enhancement in UTS is, however, correlated with a reduction in ductility, which reduces to about 4.1% for the AA6061–20% AlN_p composite, as apparently shown in Fig. 8c. Increasing the wt% of AlN_p in the composite resists the flowability of aluminium matrix and reduces the ductile aluminium alloy matrix content [26] which results in the decrease of % elongation of the composite. The mechanical properties of AA6061 matrix and AA6061 matrix reinforced with different weight percentage of AlN_p are summarized in Table 2. It is evident that the incorporation of AlN_p into AA6061 matrix significantly improves the strength of the composites.

Fig. 9a reveals the fracture surface of AA6061 matrix alloy. It shows a net work of large size dimples which indicate large

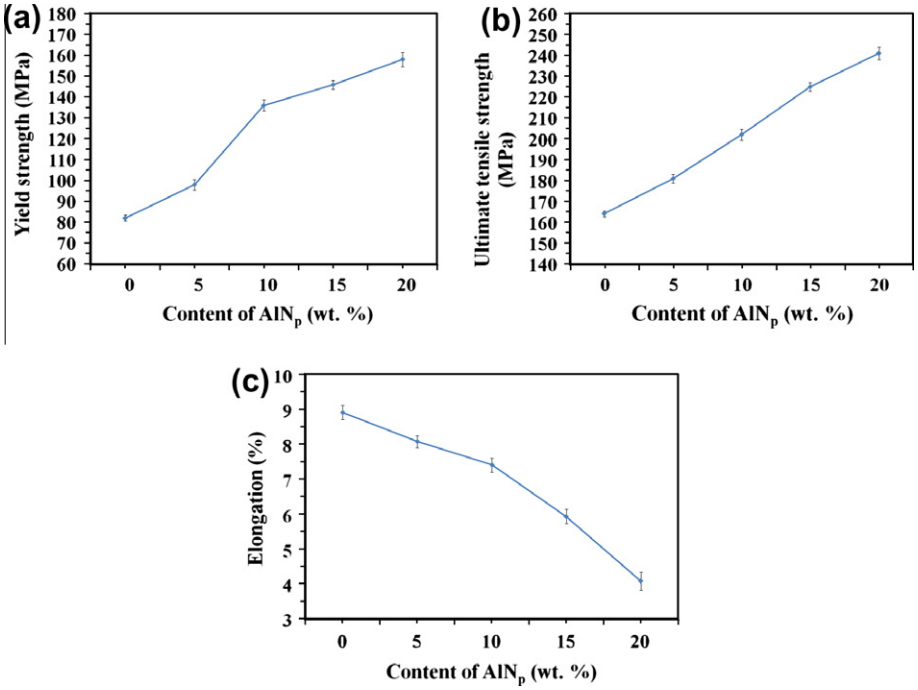

Fig. 8. Effect of weight percentage of AlN_p on (a) Yield strength, (b) ultimate tensile strength, and (c) % elongation of AA6061–AlN_p composites.

Table 2
The mechanical properties of AA6061–AlN_p composites.

S. No.	Material	0.2% Yield strength (MPa)		UTS (MPa)		Microhardness (VHN)		Macrohardness (BHN)		% Elongation	
		Ave.[a]	Std. dev.[b]	Ave.	Std. dev.	Ave.	Std. dev.	Ave.	Std. dev.	Ave.	Std. dev.
1	AA6061 matrix	82	1.53	164	1.53	44	2.15	38	1.70	8.91	0.20
2	AA6061–5% AlNp	98	2.52	181	2.08	55	2.16	45	2.22	8.07	0.17
3	AA6061–10% AlNp	136	1.53	202	2.65	68	2.27	57	1.43	7.40	0.21
4	AA6061–15% AlNp	146	2.08	225	2.08	76	2.22	66	1.99	5.93	0.21
5	AA6061–20% AlNp	158	3.46	241	3.06	91	2.20	79	1.88	4.07	0.26

[a] Average value.
[b] Standard deviation.

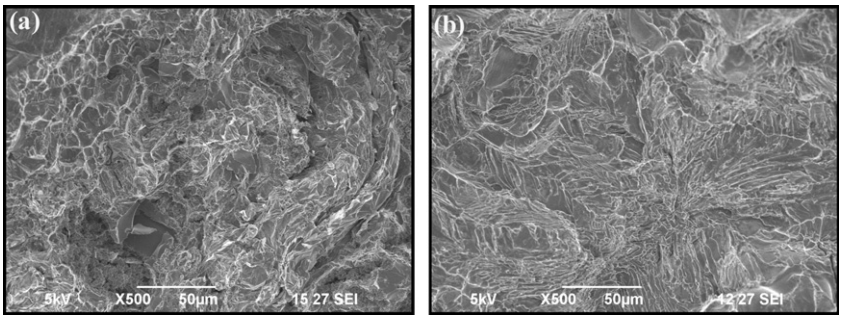

Fig. 9. Fracture surface of (a) AA6061 and (b) AA6061–20wt% AlN_p.

amount of plastic flow prior to failure. Fig. 9b reveals the fracture surface of AA6061–20% AlN_p composite. It shows a net work of dimples whose size is smaller compared to matrix alloy. The AlN_p refined the grain size of matrix alloy and reduced the ductility which resulted in smaller size dimples.

4. Conclusion

The AA6061–AlN_p composites containing different weight percentage of reinforcement viz 0%, 5%, 10%, 15% and 20% were successfully produced by stir casting method. The conclusions derived from the research work carried out are given below.

- The homogeneous dispersion of AlN_p in AA6061 matrix alloy is present.
- The good bonding and clear interface between the AlN_p reinforcement and the aluminium alloy matrix are existed.
- XRD patterns ensure the presence of AlN_p in the composites.
- UTS of the AA6061–20% AlN_p composite is 46.95% greater than the corresponding monolithic alloy.
- Higher the percentage of AlN_p reinforcement in the matrix, higher is the macrohardness and microhardness of the composite but lower is the % of elongation of the composite.

Acknowledgements

The authors wish to place their sincere thanks to the Management and Department of Mechanical Engineering, Coimbatore Institute of Technology, Coimbatore, India for extending the facilities of Welding Research Laboratory to carry out this investigation. The authors wish to register their sincere thanks for financial support rendered by Naval Research Board, DRDO, Govt. of India, vide funded project; Ref. No. DNRD/05/4003/NRB/85 dt. 30.10.2006. Authors also wish to thank Karunya University, Coimbatore, India for providing SEM, UTM testing facilities. Authors are also thankful to Mr. S.J. Vijay, Mr. I. Dinaharan, Mr. K. Kalaiselvan, Mr. M. Thambidurai, Mr. V. Rajasekaran, Mrs. V. Sarala Devi and Mr. A. Raja for their assistance offered to execute the above work.

References

[1] Speer W, Es-Said OS. Applications of an aluminum–beryllium composite for structural aerospace components. Eng Fail Anal 2004;11(6):895–902.
[2] Wang J, Yi D, Su X, Yin F, Li H. Properties of submicron AlN particulate reinforced aluminum matrix composite. Mater Des 2009;30:78–81.
[3] Hemanth J. Quartz (SiO_{2p}) reinforced chilled metal matrix composite (CMMC) for automotive applications. Mater Des 2009;30(2):323–9.
[4] Kumar GN, Narayanasamy R, Natarajan S, Babu SPK, Sivaprasad K, Sivasankaran S. Dry sliding wear behaviour of AA6351–ZrB_2 in situ composite at room temperature. Mater Des 2010;31(3):1526–32.
[5] Kaw AK. Mechanics of composite materials. 2nd ed. London New York: Taylor & Francis Group; 2006.
[6] Liu YQ, Cong HT, Wang W, Sun CH, Cheng HM. AlN nanoparticle-reinforced nanocrystalline Al matrix composites: fabrication and mechanical properties. Mater Sci Eng A 2009;505:151–6.
[7] Vicens J, Chedru M, Chermant JL. New Al–AlN composites fabricated by squeeze casting: interfacial phenomena. Composites Part A 2002;33:1421–3.
[8] Zhang Q, Chen G, Wu G, Xiu Z, Luan B. Property characteristics of a AlNp/Al composite fabricated by squeeze casting technology. Mater Lett 2003;57:1453–8.
[9] Tang YB, Liu YQ, Sun CH, Cong HT. AlN nanowires for Al-based composites with high strength and low thermal expansion. J Mater Res 2007;22:2711–8.
[10] Lii DF, Huang JL, Chang ST. The mechanical properties of AlN/Al composites manufactured by squeeze casting. J Eur Ceram Soc 2002;22:253–2561.
[11] Ellis DL, McDanels DL. Thermal conductivity and thermal expansion of graphite fiber-reinforced copper matrix composites. Metall Mater Trans A 1993;24:43–52.
[12] Couturier R, Ducret D, Merle P, Disson JP, Joubert P. Elaboration and characterization of a metal matrix composite: Al/AlN. J Eur Ceram Soc 1997;17(15,16):1861–6.
[13] Toy C, Scott WD. Ceramic–metal composite produced by melt infiltration. J Am Ceram Soc 1990;73(1):97–101.
[14] Fogagnolo JB, Robert MH, Torralba JM. Mechanically alloyed AlN particle-reinforced Al-6061 matrix composites: powder processing, consolidation and mechanical strength and hardness of the as-extruded materials. Mater Sci Eng A 2006;426:85–94.
[15] Liu ZY, Kent D, Schaffer GB. Powder injection moulding of an Al–AlN metal matrix composite. Mater Sci Eng A 2009;513–514:352–6.
[16] Lee KB, Sim HS, Kwon H. Fabrication of Al/AlN composites by in situ reaction. J Mater Sci 2006;41:6347–52.

[17] Kobashi M, Okayama N, Choh T. Synthesis of AlN/Al Alloy composites by in situ reaction between Mg_3N_2 and aluminum. Mater Trans 1997;38(3):260–5.
[18] Dyzia M, Sleziona J. Aluminium matrix composites reinforced with AlN particles formed by in situ reaction. Arch Mater Sci Eng 2008;31(1):17–20.
[19] Nassaj ET, Kobashi M, Choh T. Fabrication of an AlN particulate aluminium matrix composite by a melt stirring method. Scr Metall Mater 1995;32(12):1923–9.
[20] Wahab MN, Daud AR, Ghazali MJ. Preparation and characterization of stir cast-aluminum nitride reinforced aluminum metal matrix composites. Int J Mech and Mater Eng 2009;4(2):115–7.
[21] Hashim J, Looney L, Hashmi MSJ. Metal matrix composites: production by the stir casting method. J Mater Process Technol 1999;92–93:1–7.
[22] Gopalakrishnan S, Murugan N. Prediction of tensile strength of friction stir welded aluminium matrix TiC_p particulate reinforced composite. Mater Des 2011;32(1):462–7.
[23] Kalaiselvan K, Murugan N, Parameswaran S. Production and characterization of AA6061–B_4C stir cast composite. Mater Des 2011;32:4004–9.
[24] Hashim J, Looney L, Hashmi MSJ. Particle distribution in cast metal matrix composites – Part I. J Mater Process Technol 2002;123(2):251–7.
[25] ASTM Standard E8. Standard test method for tension testing of metallic materials. West Conshohocken (USA): ASTM, International; 2004.
[26] Dinaharan I, Murugan N, Parameswaran S. Influence of in situ formed ZrB_2 particles on microstructure and mechanical properties of AA6061 metal matrix composites. Mater Sci Eng A 2011;528:5733–40.
[27] Gupta M, Srivatsan TS. Interrelationship between matrix microhardness and ultimate tensile strength of discontinuous particulate-reinforced aluminum alloy composites. Mater Lett 2001;51:255–61.
[28] Tjong SC, Ma ZY. Microstructural and mechanical characteristics of in situ metal matrix composites. Mater Sci Eng R 2000;29(3–4):49–113.